Proceedings of the ASME 2017 Conference on Smart Materials, Adaptive Structures and Intelligent Systems
SMASIS2017
September 18-20, 2017, Snowbird, UT, USA

SMASIS2017-3840

HIGH TEMPERATURE CHARACTERIZATION OF FIBER BRAGG GRATING SENSORS EMBEDDED INTO METALLIC STRUCTURES THROUGH ULTRASONIC ADDITIVE MANUFACTURING

John J. Schomer
Department of Mechanical and Aerospace Engineering
The Ohio State University
Columbus, Ohio, 43210

Marcelo J. Dapino
Department of Mechanical and Aerospace Engineering
The Ohio State University
Columbus, Ohio, 43210
Dapino.1@osu.edu

ABSTRACT

Embedded fiber Bragg grating (FBG) sensors are attractive for in-situ structural monitoring, especially in fiber reinforced composites. Their implementation in metallic structures is hindered by the thermal limit of the protective coating, typically a polymer material. The purpose of this study is to demonstrate the embedding of FBG sensors into metals with the ultimate objective of using FBG sensors for structural health monitoring of metallic structures. To that end, ultrasonic additive manufacturing (UAM) is utilized. UAM is a solid-state manufacturing process based on ultrasonic metal welding that allows for layered addition of metallic foils without melting. Embedding FBGs through UAM is shown to result in total cross-sectional encapsulation of the sensors within the metal matrix, which encourages uniform strain transfer. Since the UAM process takes place at essentially room temperature, the industry standard acrylate protective coating can be used rather than requiring a new coating applied to the FBGs prior to embedment. Measurements presented in this paper show that UAM-embedded FBG sensors accurately track strain at temperatures higher than 400 °C. The data reveals the conditions under which detrimental wavelength hopping takes place due to non-uniformity of the load transferred to the FBG. Further, optical cross-sectioning of the test specimens shows inhibition of the thermal degradation of the protective coating. It is hypothesized that the lack of an atmosphere around the fully-encapsulated FBGs makes it possible to operate the sensors at temperatures well above what has been possible until now. Embedded FBGs were shown to retain their coatings when subjected to a thermal loading that would result in over 50 percent degradation (by volume and mass) in atmospherically exposed fiber.

INTRODUCTION

Structural health monitoring (SHM) refers to the measurement and characterization of component loading in order to determine if and when a component needs to be maintained. SHM can be performed periodically using external NDE methods to obtain data snapshots of structural load conditions, or by using sensing components that have been integrated within the structure itself. Ideal sensing candidates for SHM should have a small size in order to preserve the matrix properties of the structure, allow for straightforward real time interrogation, and provide repeatable load data. Since SHM provides a method to assess structural performance, SHM increases component reliability and decreases the necessary safety factor and material cost by allowing for proactive maintenance of critical structures. In addition to providing more meaningful load data, sensors built directly into the structure also benefit by being more resilient to external mechanical or thermal loads [1].

One type of sensor used in aerospace applications for SHM is the Fiber Bragg grating (FBG). FBG sensors consist of a grating written into the core of optical fiber that allows for a broadband input to be reflected as a specific wavelength, which can modulate based on the strain within the optical fiber to provide real time structural monitoring. FBGs are used due to their light weight, small size, and immunity to electronic interference. Modern FBG interrogation systems can obtain data from multiple sensors along the same fiber, referred to as multiplexing, allowing for seamlessly integrated sensing networks [2–5]. FBGs can obtain meaningful loading data as long as strain coupling between the structure and sensor is ensured, either by incorporating the sensor into a layer based composite structure [6–8], attaching the FBG via an epoxy externally [9–11] or by utilizing friction coupling between the structural matrix and sensor [12–15]. The latter is typically accomplished by fabricating the structure around the existing sensor, and is implemented in either layer based fiber composite builds or in additive manufacturing builds. Because FBGs are brittle and fragile, an external coating is typically used to protect them during both manufacture and operation [16]. Since FBGs are made of silica glass, they have the potential for strain sensing at higher temperatures compared with foil strain gages, and as such the focus of this study is the evaluation of embedded FBG performance at high temperatures using the industry standard acrylate coating.

The characterization of FBGs in embedded configurations focuses on the fidelity of the FBG signal, and comparison with known strain measurements. Embedding processes tend to impart residual strain on the sensor [15], and significant cross-sectional loading of the glass itself can lead to birefringence noise [17]. In order to ensure that the FBG can observe the matrix loading, there must be sufficient mechanical coupling between the sensor and matrix, which can be dependent on both the coating material and the fabrication process of the structure. This study also examines the impact of gapless encapsulation on the operating range of the protective coating, which affects impact mechanical coupling at elevated temperatures. Standard FBG interrogation assumes that the load observed by the fiber is uniform, since non-uniform loading can lead to signal distortion and error in measurements [16]. In this article, we examine the phenomenon of wavelength hopping of the FBG signal during sample heating, the ability of the sensors to track tensile loading at elevated temperatures, and the delayed thermal degradation of the acrylate coating when FBGs are embedded with the UAM process.

BACKGROUND

Embedding FBG sensors into a metallic matrix is difficult due to the brittleness of the fiber, the thermal limits of the protective coatings, and the need to embed sensors without excessive cross sectional loading. It can also be difficult to ensure that uniform strain coupling occurs between the sensor, coating, and matrix material itself. Additive manufacturing, or 3D printing, refers to techniques that involve the fabrication of structures through the addition of material. Additive manufacturing makes it possible to encapsulate a network of FBG sensors by building the structure around the sensors [18]. Some metal-based additive manufacturing techniques include selective laser melting (SLM) and ultrasonic additive manufacturing (UAM).

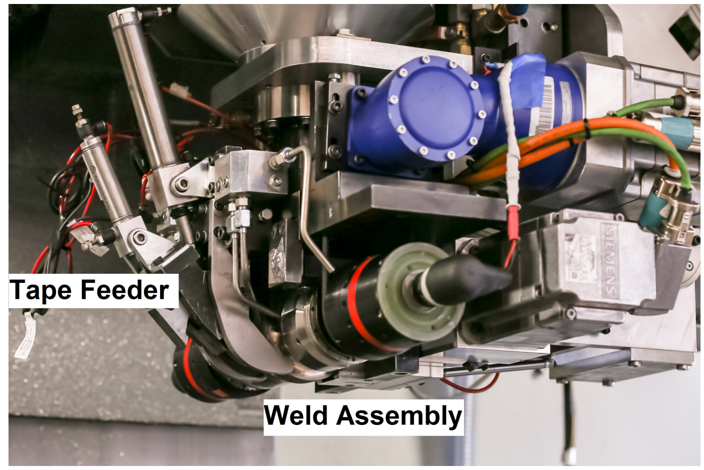

FIGURE 1. UAM SETUP. ALUMINUM TAPE IS FED TO THE ULTRASONIC WELDER WHICH BUILDS STRUCTURES ON THE BASEPLATE.

Selective laser melting is a powder based 3D printing method that relies on localized heat addition to melt layers of powder together to create a solid structure. SLM has been used to embed FBGs into metallic structures [12, 13]. In these studies, the industry standard polymer coating was removed and an electroplating layer was applied due to the heat required for the SLM process. In addition to the recoating steps, SLM FBG builds often have issues promoting uniform, gapless coating at the structure along the bottom of the FBG, due to the inability of the process to fuse powders below the FBG. In spite of this, the FBGs embedded this way are able to function as temperature sensors and provide potential for strain sensing.

Another method used to embed FBGs into metal structures is ultrasonic additive manufacturing (UAM). UAM is a layer based additive processs in which foils or tapes of similar or dissimilar metals are bonded together through ultrasonic welding. The UAM platform used in this study is a SonicLayer 4000. As Figure 1 shows, the system consists of an ultrasonic welder and metal tape feeder integrated in a CNC machine to incorporate both additive and subtractive processes. Ultrasonic welding is accomplished by colliding the asperities of two mating surfaces together at ultrasonic frequencies and high contact force. The combination of down force and ultrasonic vibrations collapses asperities at the interface between foils, disperses oxides, and promotes metallurgical welding through intimate metal to metal contact between the foils. UAM is a near-room temperature process, which allows for unprecedented capabilities in terms of

FIGURE 2. TENSILE SPECIMEN CUTOUT WITH CHANNELS FOR PLACEMENT OF FBG AND THERMOCOUPLE.

embedding temperature sensive components into metallic structures. Optical fibers have been embedded into UAM in multiple studies, and are able to retain their ability to transfer signals after encapsultaion [19, 20].

FBGs have potential for load monitoring in high temperature environments. While FBGs often make use of either polyamide or metallic coatings for higher temperature applications, there is interest in using the industry standard acrylate coating to minimize pre-processing steps. This UV cured dual-acrylate coating carbonizes at temperatures above 100 °C [21]. This carbonization process is dependent upon the content of the atmosphere in which the fiber is located, the temperature, and the rate of heating. Since UAM allows for subtractive operations in order to keep sensors in place prior to sample fabrication, and since the ultrasonic welding process occurs at low temperatures, FBGs are able to be embedded with the acrylate coating. These embedded FBGs are subject to an essentially gasless environment when totally and gaplessly encapsulated. The inhibition of acrylate coating degradation, and by extension the increase in temperature range of these sensors due to metal embedment, is a key finding of this study.

EXPERIMENTAL METHODS

Sample Fabrication

Aluminum 6061 was chosen as the matrix material due to the well-documented weldability and availability of UAM parameters for creating high-strength bonds [22]. The FBG sensors were embedded using procedures to ensure that mechanical coupling between the sensor coating and metal matrix was limited to the thermally loaded portion of the test [20]. Some specimens were fabricated with a supplemental K-type thermocouple embedded to verify internal temperatures near the FBG. After successful consolidation of the encapsulating layer of aluminum over the fiber, tensile test specimens were cut using the integrated CNC aspect of the UAM process according to ASTM E8 guidelines [23]. Figure 2 shows one of these specimens prior to the sensors being placed into the structure.

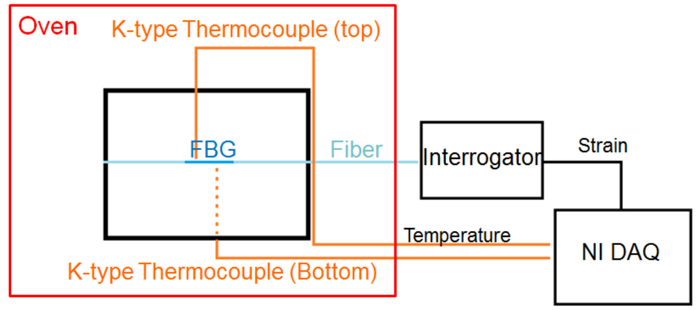

FIGURE 3. SAMPLE AND DATA ACQUISITION SETUP FOR HIGH TEMPERATURE TESTING.

Oven Testing

Test specimens were placed in an oven and loaded thermally to examine the CTE of the sensor as well as coating degradation. The samples were heated to approximately 240 °C repeatedly over a period of fifty minutes. The temperature within the structure was verified during this testing by the internal k-type thermocouple in addition to thermocouples mounted on the sample exterior. Thermocouple and FBG measurements were compiled using a NI DAQ to ensure that the measurements used the same time signal, as shown in Figure 3. The FBG signal was examined for evidence of distortion in terms of wavelength hopping due to non-linear loading [24], coupling between the sensor and matrix, and the effects of thermal expansion on the sensor. The FBGs used have a wavelength operating range of 1545 nm to 1555 nm, which correspond to +/- 4000$\mu\varepsilon$ within the fiber when the nominal wavelength is 1550 nm. By using FBGs built with a nominal wavelength of 1548 nm, the upper temperature threshold of the samples can be increased.

High Temperature Tensile Testing

High temperature tensile testing was performed using an MTS load frame with an integrated furnace. Temperature measurement was verified using external and internal thermocouple signals. The samples were loaded at a rate of 2.54 mm/min until a tensile load of 4448 N was measured in order to obtain a stress of approximately 165 MPa within the 6061 aluminum matrix to prevent yielding of the material, held at this maximum load for a time of 10 seconds, and unloaded at the same rate to the initial loading. The sample was held mechanically in place during each temperature setpoint change in order to prevent the FBG signal from going out of range of the interrogators measured reflected wavelength threshold of 1555 nm.

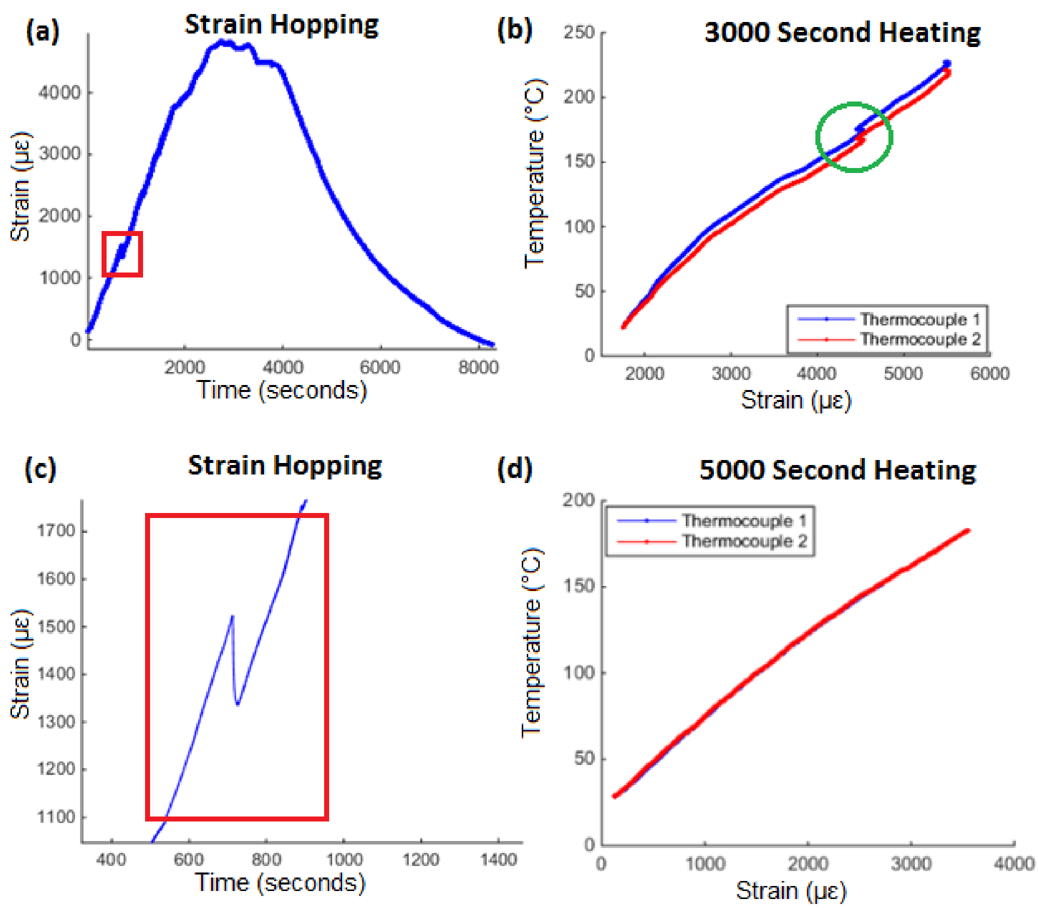

FIGURE 4. WAVELENGTH HOPPING DUE TO UNEVEN SAMPLE HEATING. (a) FBG PROFILE DURING THERMAL LOADING/UNLOADING. (b) TEMPERATURE/STRAIN CURVE WITH HOPPING. (c) DETAILED VIEW OF HOPPING REGION FROM FIGURE 4(a). (d) TEMPERATURE/STRAIN CURVE WITH NO SIGNS OF SIGNAL DISTORTION WHEN A SLOWER HEATING RATE IS USED.

Optical Evaluation

Fiber coatings were examined for signs of carbonization after elevated temperature testing. Regions of non-embedded fiber coating that had undergone carbonization were visibly charred. Test specimens were cross-sectioned, polished, and examined under an optical microscope to examine the amount of coating degradation observed after high temperature curing of the specimen. Both locations within the aluminum matrix and locations exposed to high temperature air were selected for cross sectioning. An abrasive saw was used to cut the sample prior to mounting to preserve the microstructure.

EXPERIMENTAL RESULTS

Oven Testing

During the initial rounds of thermal loading, wavelength hopping was observed, indicating non-uniform loading of the grating region. As shown in Figure 4 (a,b,c), hopping was observed during heating, but was not observed while the samples were cooling. There were no clear trends in terms of the temperature at which this shifting occurred either. When the heating was slowed down to approximately 2.4 °C per minute, seen in Figure 4 (d), there was no wavelength hopping in the data. This suggests that the distortion was due to an inconsistent thermal gradient throughout the test specimen, and is eliminated by reducing the rate of heat addition to the system which results in a more even specimen temperature.

In order to verify the temperature seen by the FBG during these thermal loadings, an internal thermocouple was character-

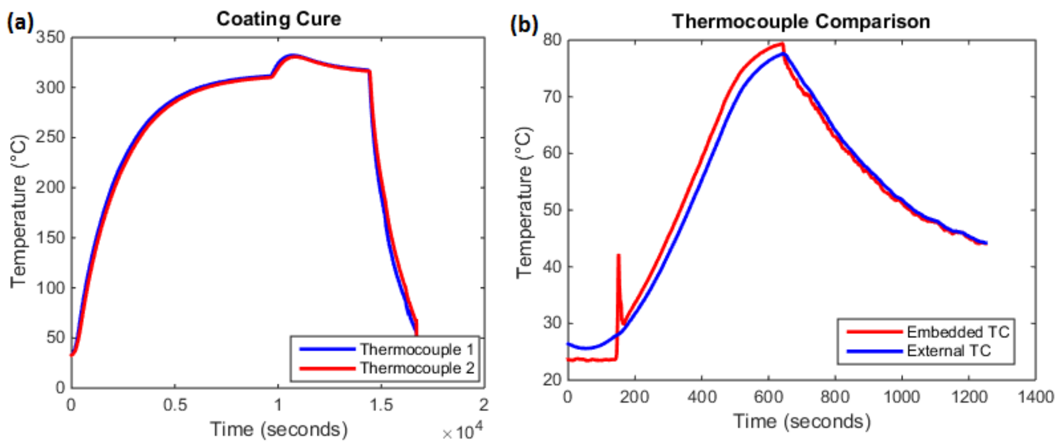

FIGURE 5. TEMPERATURE VERIFICATION AT SENSOR LOCATION. (a): TEMPERATURE/TIME PROFILE FOR SAMPLE EXAMINED FOR COATING DEGRADATION. (b): EMBEDDED TEMPERATURE SHOWN TO BE WITHIN A FEW °C OF EXTERNAL TEMPERATURE DURING OVEN TESTING.

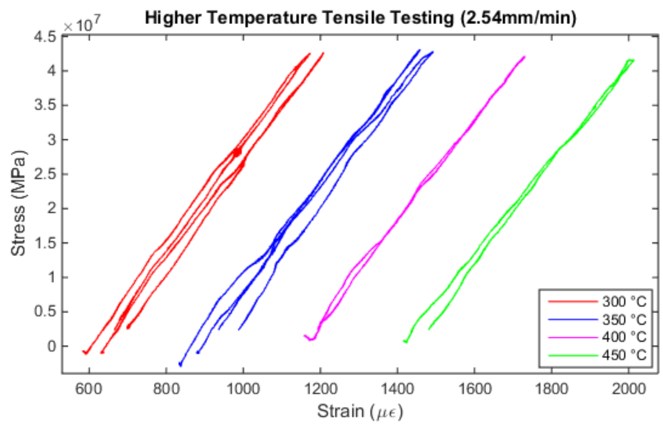

FIGURE 6. MODULUS OF ELASITICITY (SLOPE OF STRESS/STRAIN CURVE) SHOWN TO BE CONSISTENT AT ELEVATED TEMPERATURES.

ized against external thermocouple measurements in Figure 5 (b). These measurements show agreement within four °C during oven testing. Additionally, there was no observed loss of strain tracking in the FBG even after the sample was cured for three hours at 300 °C as shown in Figure 5 (a), not showing the expected degradation of over fifty percent of the acrylate coating in atmosphere [21]. This tracking confirms mechanical coupling between the sensor and metal matrix, which suggests that the coating neither degraded or melted as a result of this thermal loading.

High Temperature Tensile Testing

Samples were cyclically loaded at several constant, elevated temperatures, and the strain data observed by these FBGs is shown in Figure 6. At each temperature, the modulus of elasticity observed by the FBG was tabulated and found to be within 4 percent on average of the expected modulus of aluminum 6061, with a standard deviation of 4.6 percent, at each of the respective temperatures. These results were repeated with samples that were designed to limit the fiber-aluminum coupling to within the hot zone of the test in order to ensure that the measured strain was induced by the elevated temperature matrix material. Accurate strain tracking was shown to be repeatable at temperatures up to 450 °C. These measurements were taken when the thermocouple measurements in different locations of the furnace showed little change in temperature from the setpoint, as shown in Figure 7. This near equilibrium condition was used to ensure that the FBG waveform change was dominated by mechanical loading rather than thermal loading.

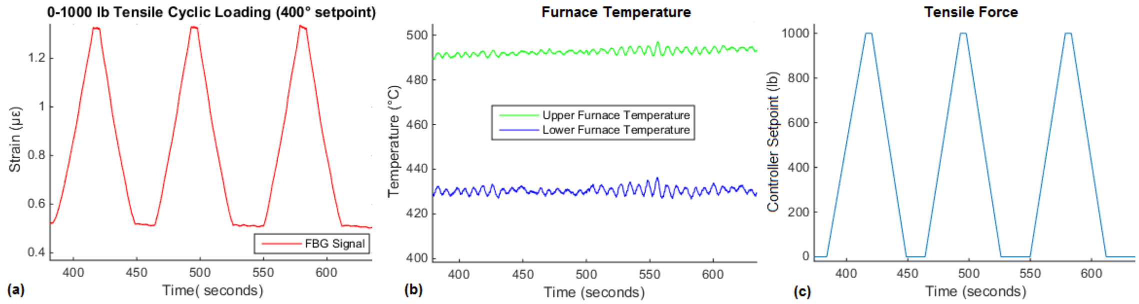

FIGURE 7. REPEATABLE STRAIN MEASUREMENTS AT HOT ZONE EQUILIBRIUM. (a) NO EVIDENCE OF HYSTERESIS OR STRAIN RATE DEPENDENCY IN STRAIN/TIME CURVE. (b) TEMPERATURE PROFILE WITHIN TEST FURNACE SHOWN TO HAVE LIMITED TIME DEPENDENCY AT HIGH TEMPERATURES. (c) INPUT FORCE PROFILE

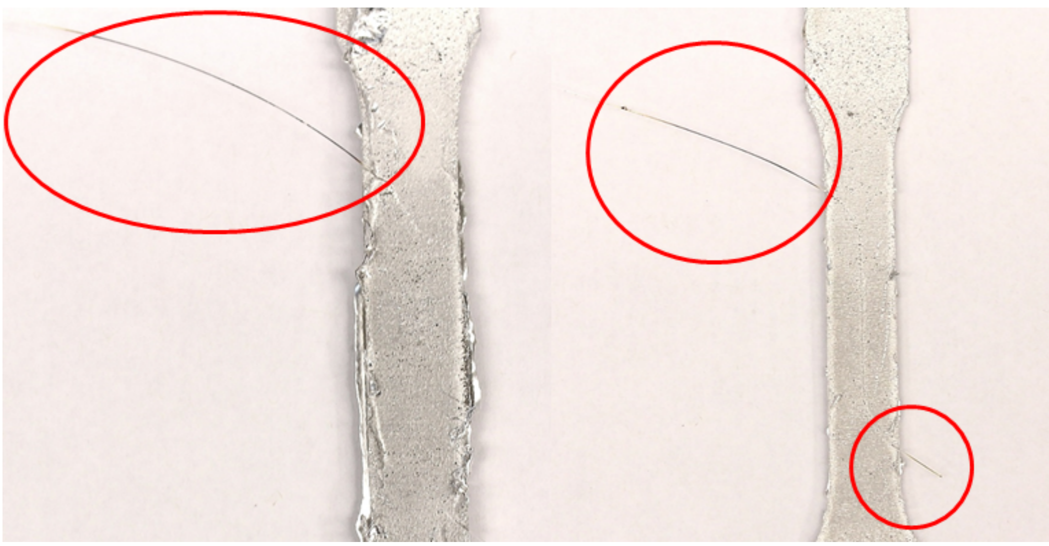

FIGURE 8. FBG COATING SUBJECTED TO CARBONIZATION OUTSIDE OF THE ALUMINUM MATRIX.

The load profile observed by the FBG is consistent with a solid coating. If the acrylate coating were melted, the resulting load profile would be proportional to the strain rate rather than the strain magnitude seen in the matrix as a result of viscous shear transfer. If this were the case, the strain value measured by the FBG would drop rapidly during the pause at maximum load during the cyclic loading, a behavior that was not observed. It is thus concluded that coupling between the matrix and sensor is not compromised by the thermal degradation of the protective acrylate coating material.

Optical Evaluation

At locations where the fiber was exposed to the hot atmosphere, the coating was almost totally degraded. This can be seen in Figure 8, where the exposed acrylate coating has a black appearance. Carbonization outside of the metal matrix was observed in all samples subjected to temperatures higher than 300 °C.

In order to study the inhibition of acrylate coating degradation as a result of UAM embedment, micrographs were taken of the sample that was exposed to the 3 hour 300 °C cure. A cross section of fiber from the atmosphere and a cross section from the embedded portion of the sample were compared in Figure 9. There are clear signs of degradation in the exposed fiber yet no signs in the embedded fiber. Since the acrylate has been shown to not be melting at high temperatures due to its strain tracking properties and the normally expected carbonization process is inhibited, this result shows that the operating range of acrylate coated FBGs as structural sensors has been improved as a result of the UAM embedding process.

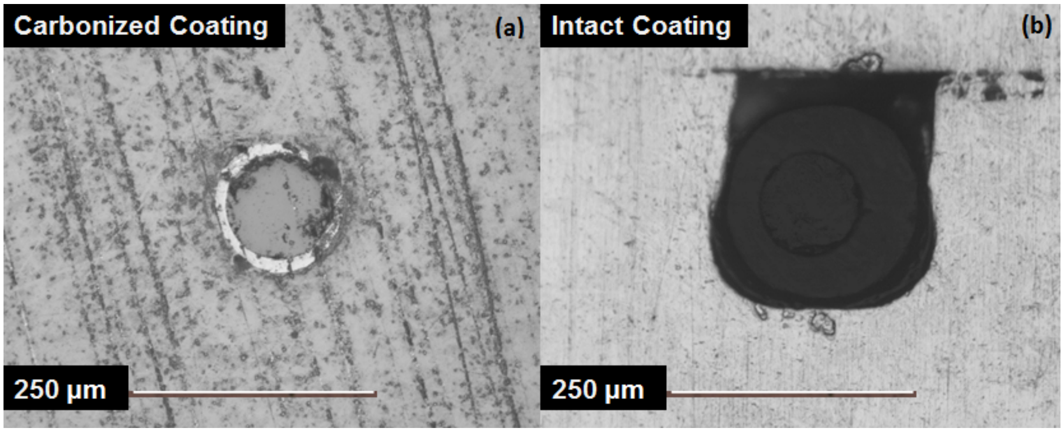

FIGURE 9. DEGRADATION OF ACRYLATE COATING INHIBITED BY METAL ENCAPSULATION. (a) EXPOSED COATING SUBJECTED TO NEAR TOTAL CARBONIZATION. (b) NO DEGRADATION OBSERVED IN EMBEDDED COATING.

Concluding Remarks

UAM was used to embed acrylate coated FBGs in order to characterize their performance at high temperatures. The areas of interest in this study were the fidelity of the signal in terms of providing repeatable strain tracking while minimizing wavelength hopping and the inhibition of coating degradation in order to increase the operating range of acrylate coated FBGs. Accurate and repeatable strain tracking was observed in FBG sensors embedded in aluminum 6061 at temperatures up to 450 °C. The embedded acrylate coatings showed no signs of thermoxidative degradation even after large thermal loads were applied to the sensors, which confirms the inhibitive aspect of gapless metal encapsulation on this reaction. These results show that embedded FBG sensors with acrylate coatings can be used for structural health monitoring in high temperature environments.

ACKNOWLEDGMENT

The authors wish to acknowledge the member organizations of the Smart Vehicle Concepts Center, a National Science Foundation Industry/University Cooperative Research Center established under grant IIP-1238286 (www.SmartVehicleCenter.org), and the technical and in-kind support from Insensys Ltd.

REFERENCES

[1] Huston, D., 2010. *Structural sensing, health monitoring, and performance evaluation*. CRC Press.

[2] Kuang, K., and Cantwell, W., 2003. "Use of conventional optical fibers and fiber bragg gratings for damage detection in advanced composite structures: a review". *Applied Mechanics Reviews,* ***56***(5).

[3] Childs, P., Wong, A., Gowripalan, N., and Peng, G., 2007. "Measurement of the coefficient of thermal expansion of ultra-high strength cementitious composites using fibre optic sensors". *Cement and Concrete Research,* ***37.5***.

[4] Bayo, E., and Leka, L., 1989. "A close look at the embedment of optical fibers into composite structures". *Journal of Composites, Technology and Research,* ***11.3***.

[5] Felli, F., Paolozzi, A., Vendittozzi, C., Paris, C., and Asanuma, H., 2016. "Use of fbg sensors for health monitoring of pipelines". In SPIE Smart Structures and Materials+ Nondestructive Evaluation and Health Monitoring, International Society for Optics and Photonics, pp. 98031L–98031L.

[6] Pan, X., Liang, D., and D.Li, 2006. "Optical fiber sensor layer embedded in smart composite material and structure". *Smart materials and structures,* ***15***(5), p. 1231.

[7] Foedinger, R., Rea, D., Sirkis, J., Baldwin, C., Troll, J., Grande, R., Davis, C., and Vandiver, T., 1999. "Embedded fiber optic sensor arrays for structural health monitoring of filament wound composite pressure vessels". In 1999 Symposium on Smart Structures and Materials, International Society for Optics and Photonics, pp. 289–301.

[8] Roberts, S., and Davidson, R., 1991. "Mechanical properties of composite materials containing embedded fiber-optic sensors". In OE Fiber-DL tentative, International Society for Optics and Photonics, pp. 326–341.

[9] Arsenault, T., Achuthan, A., Marzocca, P., Grappasonni, C., and Coppotelli, G., 2013. "Development of a fbg based distributed strain sensor system for wind turbine structural health monitoring". *Smart Materials and Structures,* ***22***(7), p. 075027.

[10] Kinet, D., Mégret, P., Goossen, K., Qiu, L., Heider, D., and Caucheteur, C., 2014. "Fiber bragg grating sensors toward structural health monitoring in composite materials: Challenges and solutions". *Sensors,* ***14***(4), pp. 7394–7419.

[11] Vorathin, E., Hafizi, Z., Ghani, S., and Lim, K., 2016. "Real-time monitoring system of composite aircraft wings utilizing fibre bragg grating sensor". In IOP Conference Series: Materials Science and Engineering, Vol. 152, IOP Publishing, p. 012024.
[12] Stoll, P., Matthew, J., Spierings, A., Bauer, T., Wegener, K., and Maier, R., 2016. "Embedding fibre optical sensors into slm parts". In Proceedings of the 27th Annual International Solid Freeform Fabrication Symposium, pp. 1815–1825.
[13] Havermann, D., Matthew, J., MacPherson, W., Hand, D., and Maier, R., 2015. "Measuring residual stresses in metallic components manufactured with fibre bragg gratings embedded by selective laser melting". In International Conference on Optical Fibre Sensors (OFS24), International Society for Optics and Photonics, pp. 96340T–96340T.
[14] Maier, R., MacPherson, W., Barton, J., Carne, M., Swan, M., Sharma, J., Futter, S., Knox, D., Jones, B., and McCulloch, S., 2013. "Embedded fiber optic sensors within additive layer manufactured components". *IEEE Sensors Journal,* ***13***(3).
[15] Kantaros, A., and Karalekas, D., 2013. "Fiber bragg grating based investigation of residual strains in abs parts fabricated by fused deposition modleing process". *Materials and Design,* ***50***(44).
[16] Kashyap, R., 1999. *Fiber Bragg Gratings*. Academic press.
[17] Okamoto, K., Hosaka, T., and Edahiro, T., 1981. "Stress analysis of optical fibers by a finite element method". *IEEE Journal of Quantum Electronics,* ***17.10***.
[18] Wong, K., and Hernandez, A., 2012. "A review of additive manufacturing". *ISRN Mechanical Engineering*.
[19] Mou, C., Saffari, P., Li, D., Zhou, K., Zhang, L., Soar, R., and Bennion, I., 2009. "Smart structure sensors based on embedded fibre bragg grating arrays in aluminium alloy matrix by ultrasonic consolidation". *Measurement Science and Technology,* ***20.3***.
[20] Schomer, J., Hehr, A., and Dapino, M., 2016. "Characterization of embedded fiber optic strain sensors into metallic structures via ultrasonic additive manufacturing". In SPIE Smart Structures and Materials+ Nondestructive Evaluation and Health Monitoring, International Society for Optics and Photonics, pp. 980320–980320.
[21] Stolov, A., Simoff, D., and Li, J., 2008. "Thermal stability of specialty optical fiber". *Journal of Lightwave Technology,* ***26.20***.
[22] Wolcott, P., Hehr, A., and Dapino, M., 2014. "Optimized welding parameters of al 6061 ultrasonic additive manufactured structures". *Journal of Materials Research,* ***29***(18).
[23] Standard, A. E8/e8m, 2009. standard test methods for tension testing of metallic materials. astm international, west conshohocken pa; 2009. doi: 10.1520. Tech. rep., E0008-E0008M-09, www. astm. org.
[24] Webb, S., Peters, K., Zikry, M., Vella, T., Chadderdon, S., Selfridge, R., and Schultz, S., 2011. "Wavelength hopping due to spectral distortion in dynamic fiber bragg grating sensor measurements". *Measurement Science and Technology,* ***22.6***(065301).